Fatigue crack initiation and propagation behaviour of a squeeze cast Al alloy and its statistical aspect

M. Goto[1], T. Yamamoto[1], H. Nisitani[2] & N. Kawagoishi[3]
[1]*Dept. of Mechanical Engineering, Oita University, Japan*
[2]*Kyushu-Sangyo University, Japan*
[3]*Kagoshima University, Japan*

Abstract

In order to clarify the crack initiation and propagation behaviour of a squeeze cast aluminum-silicon-magnesium alloy, fatigue tests of smooth specimens cut from Al alloy car wheels formed by the squeeze casting were carried out under the constant stress amplitudes. The behaviour of a major crack was monitored successively by the plastic replication method. In addition to this, the analysis of the initiation and propagation behaviour of multiple cracks were made to investigate the statistical characteristics of microcracks. Namely, the distribution of crack initiation life, propagation life, crack growth rate and crack length were studied by assuming Weibull distribution. Through the values of Weibull parameters and coefficient of variance, the statistical characteristics were discussed quantitatively.

1 Introduction

Although aluminum casting alloys have been widely used for the machines and structures, alloys usually show a low fatigue strength and a low reliability caused from the casting defects. The squeeze casting [1,2] has dramatically improved the mechanical properties, fatigue characteristics and reliability of the strength of aluminum casting alloys. Recently, many fatigue data of squeeze cast Al alloys have been reported, however there are a few data concerning the behaviour of small cracks [3] which nearly control the fatigue life of plain members.

In the present study, fatigue tests of smooth specimens cut from squeeze cast Al alloy car wheels were carried out to clarify the initiation and propagation behaviour of a major crack which led to the final fracture of the specimen. To minimize the scatter in fatigue tests due to the fluctuation of laboratory atmosphere, the machine was placed in a small cabin in the laboratory. The temperature and humidity in the cabin were kept under control (t = 30℃, h = 60%). All the tests were made in controlled air. Three pieces of a region whose area is 4mm^2 (2×2mm) were set on the surface of a specimen to clarify the statistical aspects for fatigue behaviour. In addition to a major crack, the behaviour of all cracks initiated within these regions was monitored by a plastic replica technique. Statistical characteristics of fatigue cracks were analysed by assuming a Weibull distribution. Namely, the distribution of crack initiation life, propagation life, crack growth rate and crack length were represented. Through the values of Weibull parameters and coefficient of variance, the statistical characteristics were discussed quantitatively.

2 Experimental procedures

The material was an aluminum-silicon-magnesium casting alloy (JIS: AC4CH). The material was cut from the thick portions (thickness: 15mm) of car wheels formed by a vertical squeeze-casting machine. After the casting, all the wheels were solution treated, followed by ageing. The mechanical properties after the heat treatment were 214 MPa 0.2% proof stress, 263 MPa ultimate tensile strength, 337 MPa true breaking stress, and 27.3% reduction of area.

The round bar specimens with 5mm diameter were machined from the bars cut from the car wheels. Although the specimens have a shallow circumferential notch (depth = 0.25mm, radius = 20mm), the strength reduction factor for this geometry is close to unity, so that the specimens can be considered as plain specimens. Before testing, all the specimens were electropolished to remove about 20μm from the surface layer, in order to facilitate the observations of changes in the surface state.

All the tests were carried out using a rotating bending fatigue machine with a capacity of 100 Nm operating at 50 Hz. The specimens were fatigued at the room temperature in air under the constant stress amplitude. To minimize the effect of fluctuation of atmosphere on the fatigue data, the machine was placed in a small cabin in the laboratory. The temperature and humidity in the cabin were kept under control; t = 30℃, h = 60%.

The observation of fatigue damage on the surface and the measurements of crack length were made via plastic replicas using an optical microscope at a magnification of ×400. The value of stress, σ_a, means the nominal stress amplitude at the minimum cross section.

3 Experimental results and discussion

3.1 Crack initiation and propagation behaviour

Figure 1 shows the S-N curve in uncontrolled air. The ○ and ● symbols show the experimental data gathered in summer- and winter-season, respectively. The influence of atmosphere on fatigue strength is clearly recognized. Fig.2 shows

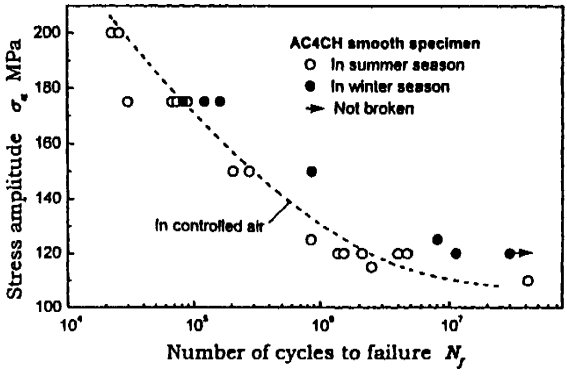

Figure 1: S-N data in uncontrolled laboratory air.

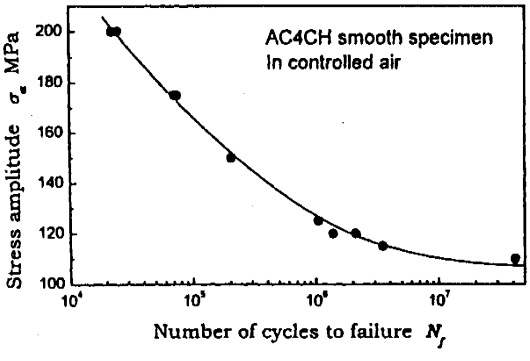

Figure 2: S-N data in controlled laboratory air.

the S-N curve in controlled laboratory air (t = 30°C, h = 60%). Scatter in the fatigue strength is dramatically decreased when compared to the uncontrolled air (Fig.1). The fatigue limiting stress at 10^7 cycles is σ_w = 110MPa in the controlled atmosphere. To minimize the scatter in the fatigue data due to the fluctuation of laboratory atmosphere, all the tests were carried out in controlled laboratory air.

The normalized S-N curve (σ_a/σ_u vs N_f relation) was compared to the curve for a forged Al alloy 6061-T6 (Al-Si-Mg alloy) [4]. The tensile strength of

6061-T6 was σ_u = 309MPa which is larger than AC4CH: σ_u = 263MPa. There were negligible differences in the σ_a/σ_u vs N_f relation. Thus, it can be concluded that the fatigue strength of squeeze cast Al alloy cut from the car wheel is comparable to the forged 6061-T6 alloy. This may relate to that the specimens were cut from thick portion of the wheels where includes few defects. This indicates that the present data never represent the fatigue strength for actual car wheel, however it may be applicable for the estimation of the standard fatigue characteristics of the material used for wheel.

The initiation and growth behaviour of microcracks was monitored by the plastic replication technique. Results showed that, at an early stage of cycling, fatigue cracks were initiated at or near the interfaces between the matrix and eutectic Si particles. Some cracks were initiated from a slip band in the matrix, however no cracks initiated from the defects such as pinholes and shrinkage porosities were observed. After the initiation, the crack grew with the influence of the microstructure.

Figure 3 shows the *dl/dN* vs. *l* relation. Here, the crack growth rate, *dl/dN*, was calculated from the crack growth curves represented by smoothed curves which pass through the average of each set of plots. For all the stress amplitudes, the change in the relation occurs at around l = 0.3mm. Namely, the relation for l > 0.3mm can be approximated by the straight line. Its slope is about unity when $\sigma_a \gtrsim$150MPa. On the other hand, the relation for l < 0.3mm is accelerated from the extension of relation for large crack (l > 0.3mm). This acceleration comes from the difference in the crack growth mode, i.e., dominant growth mode tends to change from shear to tensile mode at $l \cong$ 0.3mm.

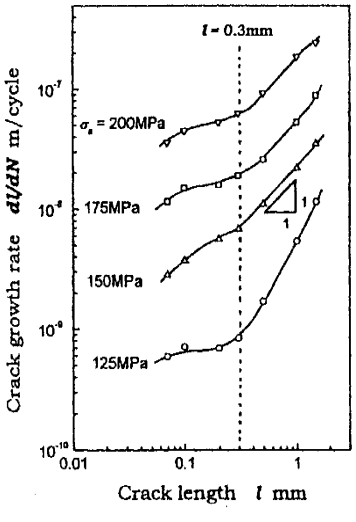

Figure 3: *dl/dN* vs *l* relation for major cracks.

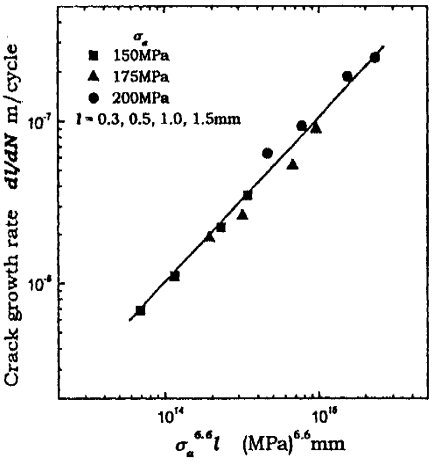

Figure 4: *dl/dN* vs $\sigma_a^n l$ relation (n = 6.6).

Figure 4 shows the dl/dN vs. $\sigma_a^n l$ relation [5], here n is the material constant and is about 6.6. The growth rate of a crack larger than 0.3mm under a large stress ($\sigma_a \gtrsim$150MPa) is determined by a small crack growth law.

3.2 Statistical characteristics of fatigue behaviour

In order to clarify the statistical characteristics of small cracks in carbon steels, Goto et.al. [6] analysed the behaviour of all the cracks initiated within the specific region. In the present alloy, three pieces of a region whose area is 4mm^2 (2×2mm) were set at regular intervals on the replicas gathered from the midsurface of a specimen, then the initiation and propagation behaviour of all the microcracks in the regions were analysed.

Figure 5 shows the growth data (the ln$l$ vs. N/N_f relation) of all the cracks within the observed regions. The acceleration, deceleration and temporary arrest of crack growth are recognized. The ●-symbol indicates the growth data of a major crack. When comparing the initiation time of 0.01mm crack, the value of N/N_f is about 0.1 to 0.2 at a high stress and it is beyond 0.4 at a low stress. After the initiation of the first crack, many cracks are initiated continuously, however no initiation of a newly crack is recognized in the range $N/N_f > 0.7$ at $\sigma_a \geqq$ 150MPa and $N/N_f > 0.9$ at σ_a = 120MPa.

Figure 6 shows the crack density δ, the number of cracks in unit area (1 mm^2), vs N/N_f relation. The crack density increases with an increase in cycling, however it tends to decrease in the later stages of cycling ($N > 0.7N_f$). The starting time of decrease in δ is nearly equivalent to the time when the newly initiation of crack was ceased. In addition to this, the coalescent of cracks makes decrease the value of δ in the later stages of cycling.

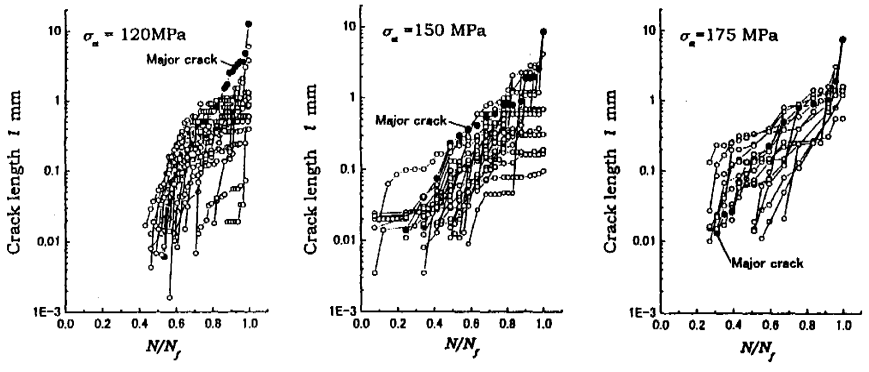

(a) σ_a = 120MPa (b) σ_a = 150MPa (c) σ_a = 175MPa

Figure 5: Growth data of all the cracks initiated within the observed regions.

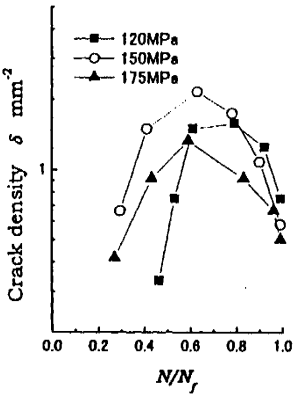

Figure 6: Crack density, δ, vs N/N_f relation.

Figure 7 shows the transition of crack length distribution. When the value of N/N_f increases from 0.41 to 0.63, both the crack length and the number of cracks increase. However, the number of cracks decreases while N/N_f changes from 0.63 to 0.78 ($\Sigma n = 26 \rightarrow 22$, n: number of cracks). On the other hand, 17 cracks out of 18 cracks at $N/N_f = 0.41$ are smaller than 0.1mm. At $N/N_f = 0.78$, however, the lengths of 22 cracks are distributed over 0.03 to 1.0mm. Namely, the increase in the range of crack length is remarkably large, whereas the increase in the number of cracks is not so large. This indicates that the crack growth behaviour is strongly affected by the interaction of microstructure and other cracks.

Since fatigue data include large scatter, the distribution properties must be analysed to estimate the scatter characteristics quantitatively. Many studies concerning the statistical treatment of fatigue life and crack length have been performed, and these suggest that a log-normal distribution or Weibull distribution is suitable for analysis of such fatigue data. In what follows, the distribution studies of each data set were performed using three-parameter Weibull distribution function $F(x)$ expressed by the following equation:

$$F(x) = 1 - \exp\left[-\left(\frac{x-\gamma}{\eta}\right)^m\right] \tag{1}$$

Here, the three constants m, η and γ are the shape parameter, scale parameter and location parameter, respectively. The determination of three Webull parameters was made using a correlation factor method proposed by Sakai and Tanaka [7].

Figure 8 shows the distribution of 0.02mm crack initiation life, N_i, represented on Weibull probability paper. Crack initiation life can be represented by a three- parameter Weibull distribution.

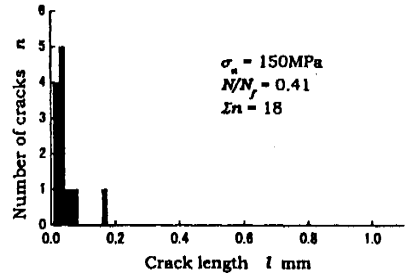

(a) N/N_f = 0.41

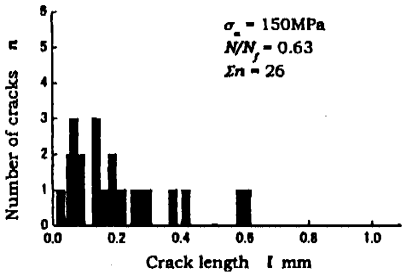

(b) N/N_f = 0.63

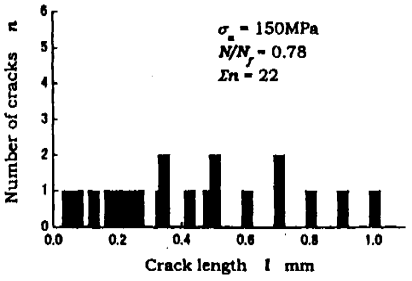

(c) N/N_f = 0.78

Figure 7: Transition of crack length distribution due to the cycling.

The distribution for various phases of crack propagation life, $N_{0.02\to0.1}$, $N_{0.1\to0.3}$, $N_{0.3\to1.0}$ and $N_{0.02\to1.0}$ were studied. Here, the terms $N_{0.02\to0.1}$, $N_{0.1\to0.3}$, $N_{0.3\to1.0}$ and $N_{0.02\to1.0}$ are the crack propagation lives from 0.02 to 0.1mm, 0.1 to 0.3mm, 0.3 to 1.0mm and 0.02 to 1.0mm, respectively. Results showed that the three-parameter Weibull distribution holds for each lifetime.

Figure 9 shows (a) the crack growth rates distribution at three crack lengths (l = 0.05, 0.1 and 0.5mm) plotted on Weibull probability paper, and (b) the log-normal probability paper. The straight lines in Fig.9(b) are the distribution

functions calculated by the least squares method. The distribution of small-crack growth rate is expressed by both the Weibull and log-normal distribution. It should be noted, however, that for large population samples one of these function is likely to describe the extreme probabilities more accurately.

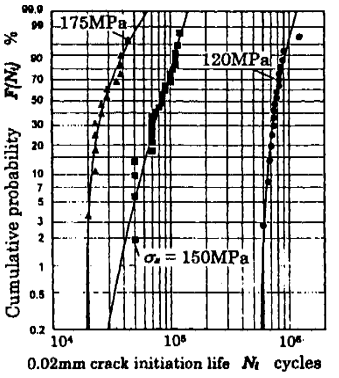

Figure 8: Distribution of 0.02mm crack initiation life.

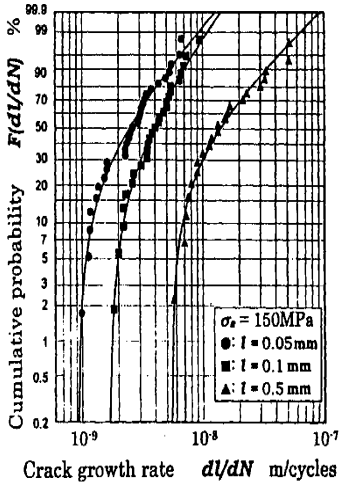

(a) Weibull distribution paper

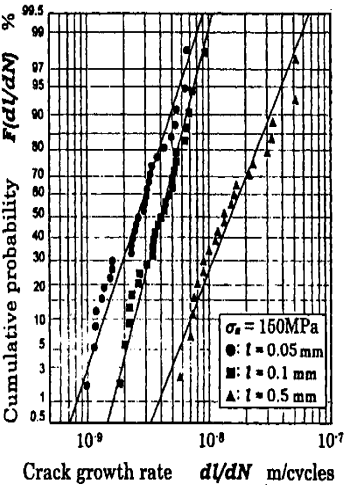

(b) Log-normal probability paper

Figure 9: Distribution of *dl/dN* for 0.05, 0.1 and 0.5mm cracks (σ_a = 150MPa).

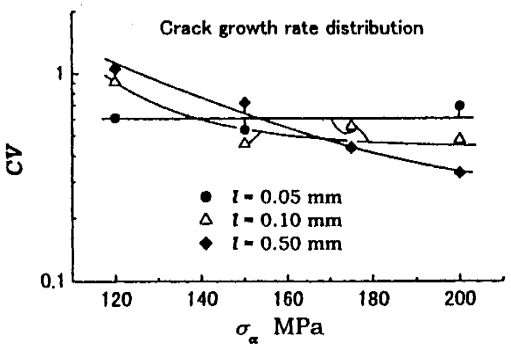

Figure 10: *CV* vs σ_a relation for crack growth rate distribution.

Further statistical investigation is therefore required to evaluate the most applicable function such that the low probability regime (at the edge of the distribution) can be predicted more accurately.

Figure 10 shows the coefficient of variance, *CV*, vs stress amplitude relation, here $CV = s/\mu$, s is the standard deviation and μ is the mean value. For 0.05mm crack, no distinct stress dependency of *CV* value is recognized. For 0.1 and 0.5mm cracks in $\sigma_a < 150$MPa, *CV* decrease sharply with an increase in σ_a . In $\sigma_a > 150$MPa, the decrease in *CV* becomes milder, then it tends to saturate to each specific *CV* value; $CV = 0.5$ for 0.1mm crack and 0.3 for 0.5mm crack.

Figure 11 shows the *dl/dN* vs *l* relation. Symbol ○ means the average value of *dl/dN* calculated from all the cracks initiated within the observed region, and ● is for major cracks. The average values show the similar trend with major cracks. Thus, the growth rate of major crack is not necessarily large when comparing the average *dl/dN* of all the cracks.

Fatigue damage is usually evaluated through the change in surface morphology such as crack length. The length of cracks initiated at both the same stress amplitude and same number of cycles exhibits large scatter. This indicates that the crack length distribution must be clarified to ensure the reliability of fatigue damage estimated based on the crack length.

Figure 12 shows the crack length distribution at each relative number of cycles. Three-parameter Weibull distribution is useful for representing the crack length distribution.

Figures 13 and 14 show the m vs N/N_f and η vs N/N_f relations, respectively. The value of m takes nearly unity independent of both the stress amplitude and number of cycles. On the other hand, the η vs N/N_f relation is represented by a linear relation independent of the stress amplitude.

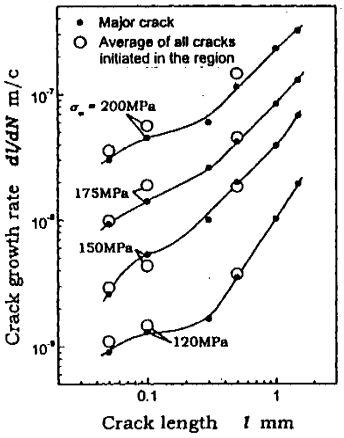

Figure 11: Average dl/dN vs l relation for all the cracks within the region.

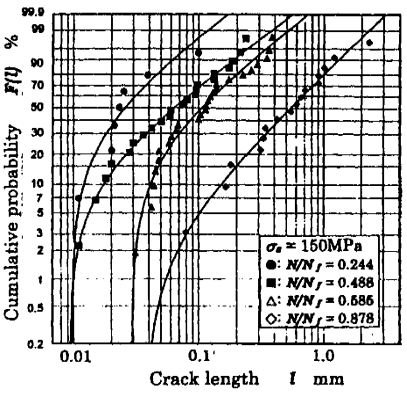

Figure 12: Crack length distributions at various N/N_f (σ_a = 150 MPa).

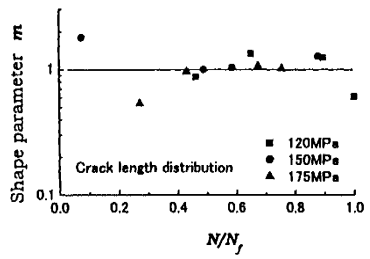

Figure 13: m vs N/N_f relation.

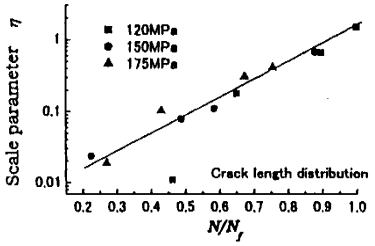

Figure 14: η vs N/N_f relation.

4 Conclusions

The main conclusions may be summarized as follows:

1. The fatigue strength based on the tensile strength σ_u is comparable to a forged 6061-T6 alloy (Al-Si-Mg alloy). This may relate to that the specimens were cut from the thick parts of the wheels where include few defects.
2. Fatigue cracks were initiated principally from the eutectic Si particles and sometimes from a slip band in the matrix. But, no initiation from microscopic defects such as pinholes and shrinkage porosities was observed.
3. After the crack initiation, the shear mode growth controlled the growth behaviour of microcracks and shear mode cracks were apt to be influenced by the microstructure. For large cracks (l > 0.3mm), however, the predominant growth mode was the tensile mode

4. When the stress is relatively high ($\sigma_a \gtrsim$ 150MPa), *dl/dN* of a crack larger than 0.3mm was determined uniquely by a term $\sigma_a^n l$ ($n = 6.6$).
5. For a range $N < 0.7N_f$, the crack density, δ, increased with an increase in N. After the value of N exceeded $0.7N_f$, however, δ tended to decrease with an increasing N.
6. The crack initiation life, crack propagation life and crack length were represented by the Weibull distribution. With regard to the crack length distribution, the shape parameter takes about unity independent of both the stress amplitude and number of cycles, whereas the linear relation for the η, scale parameter, vs N/N_f relation holds independent of the stress amplitude.
7. The distribution of small crack growth rate was expressed by both the log-normal and Weibull distribution plots.

References

[1] Kaneko, Y., Murakami, H., Kuroda, K. & Nakazaki, S., Squeeze casting of aluminum. *Foundry Trade Journal*, **28**, pp. 397-411, 1980.

[2] Williams, G., Squeeze form combines casting with forging. *Foundry Trade Journal*, **2**, pp. 66-70, 1984.

[3] Goto, M., Yamamoto, T., Nisitani, H. & Kawagoishi, N., Crack initiation and growth behaviour of smooth specimens cut from the squeeze cast Al alloy car wheels. *ECF14 Fract. Mech. Betond 2000*, 1, eds. A. Neimitz, I.V. Rokach, D. Kocanda & K. Golos, EMAS Publ., pp. 623-630, 2002.

[4] Goto, M. & DuQuesnay, D.L., Fatigue bahaviour of 6061-T6 aluminum alloy plain specimens. *SAE Tech. Paper Series*, No.970703, Soc. Automotive Engng-USA, pp. 1-7, 1997.

[5] Nisitani, H., Goto, M. & Kawagoishi, N., A small crack growth law and its related phenomena. *Eng. Fract. Mech.*, **41(4)**, pp. 499-513, 1992.

[6] Goto, M., Statistical investigation of the behaviour of microcracks in carbon steels. *Fatigue Fract. Eng. Mater. Struct.*, **14(8)**, pp. 833-845, 1991.

[7] Sakai, T. & Tanaka, T., Estimation of three parameters of Weibull distribution for carbon steels. *J. Jpn. Soc. Mater. Sci.*, **29**, pp. 17-23, 1980.